On Simplifications in the Technical Vision Algorithm

Yuliya Gerasimova[1], Alexander Titov[2], Boris Shumilov[2]
1. Povolzhskiy State University of Telecommunication and Informatics, Samara, Russia
2. Tomsk State University of Architecture and Building, Tomsk, Russia
E-mail: sbm05@yandex.ru

Abstract: The purpose of the work is creation of a new technology for recognition of transport infrastructure facilities, including simplifications of algorithm for operation of technical facilities from video fixing under changing environmental factors. In this work, we used methods for determining the volume of three-dimensional facilities from the data of photo and video recording of the surrounding situation. The novelty of the research is building of decision algorithms based on devices and sensors that recognize changing road conditions, namely, defects in coverage. We obtained the algorithm of technical vision, which is supposed to implement as a program on a mobile device for recognition of transport infrastructure facilities and their defects by means of stereometry. One could use the data obtained in the planning of road repairs, in the analysis of traffic accidents by road police, for processing road users' complaints, etc.
Keywords: highways, pavement defects recognition, mobile technologies, laser scanning, photogrammetry, calibration, binarization, edge detection

1. Introduction

Automation of diagnostics of road surface condition represents an urgent challenge, as economic losses caused by late detection of cracks and potholes are becoming increasingly significant. The rapid growth in the number of automotive vehicles in Russia and the world is many times ahead of the pace of road construction. As a result, the road network operates in stressed conditions. The condition of highways, the quality of the road bed surface, the visibility, the width of the roadway, the arrangement of the relevant signs have a significant impact on road safety and define the concept of "road conditions" in their totality. The trajectory and speed of the automobile depends on the "road conditions". In investigation of road traffic accidents, as experts believe, the impact of road conditions on occurrence of road accidents is from 60 to 80% of cases [1]. The procedure for fixing and registration of accidents currently provides three options: 1) the European Protocol, the participants in the incident themselves draw up and record all the circumstances, with the obligatory use of photo and video equipment; 2) the emergency commissioner draws up and records all the circumstances of the incident, with the obligatory use of photo and video equipment; 3) the traffic police inspector draws up and records all the circumstances of the incident, the use of photo and video equipment is not mandatory. Quite often, there are controversial situations, the investigation and examination of which we carry out on the available materials, including photographs and video filming. In most cases, the participants of the incident use the mobile devices when fixing and registering the situation (figure 1). In figure 1, a, the driver of the motorcycle recorded the overall traffic situation. In figure 1, b in order to understand the scale and size of the potholes, the driver used the glove as a scale marker. In this situation, the owner of the motorcycle will have to prove that the road surface does not meet the requirements for the operational condition, acceptable under the terms of road safety.

a) b)

Figure 1. Photos of potholes in the road surface

The key component in implementation of fully mobile devices capable of performing tasks of collecting road data is the technical vision system [2-3]. Development of automatic diagnostic systems for evaluation of defects and detection of destructions of the road surface is possible with the use of video cameras and image processing algorithms. However, the problem of the operation of systems based on pure video is their inability to filter out such shadings in pictures as road marking elements, smudges from oil and lubricant spills, brake traces, shadows of passing cars, and fresh patches [4]. One of the classical methods of extracting information about the depth of a three-dimensional (3D) object is the method of photogrammetric processing of stereoscopic images of a 3D object obtained from different angles [5-6]. The drawback of traditional digital photogrammetry is the significant involvement of the human operator, as well as the need to pre-scan analog images using high-precision scanners. The mobile laser scanning-based systems have become a breakthrough in road condition diagnostics [7] (figure 2). However, high cost of this technology has made things more complicated. The use of modern inexpensive photogrammetric methods [8-10] to determine damages and unevenness of the road surface and structural elements of the road gives a new impetus to the development of digital technologies for the design of road repairs, increasing mobility and lowering the cost of the works.

Figure 2. Laser scanning points includes reflections from people, machinery, vegetation, etc.

The presented report exams the problem of automating the diagnosis of the current state of roads. Using the availability and prevalence of mobile devices, we proposed to use mobile measurements on a series of consecutive frames of video shooting. This is because with the development of modern methods of analysis and recognition of objects from their images, the accuracy of calculating the characteristics of these objects, namely, area and volume, increases. Additionally, this will reduce the likelihood of overstatement of road works when planning repairs. As parts of this report there will be: 1) the task of automating the recognition of damage to the road surface; 2) description of the methods of linear perspective and the construction of the projective matrix; 3) the possibility of applying a linear perspective to solve the problem; 4) description of the methods of "external calibration" of a video camera and the results of numerical experiments. In addition, we will try to present the advisability of reducing the number of measured points for referencing stereo images using preliminary calibration of the internal parameters of the camera; and also the possibility of pre-binarization of the image using a variety of algorithms. We describe numerical experiment on the use of the detector of characteristic points of the image and we make appropriate conclusions.

2. Research methods

The solution of the problem is reduced to the formation of geometric transformations according to the graphic labels of the elements of the matrix and the restoration of the three-dimensional coordinates of the points of the object along perspective projections in each picture plane [11] (figure 3). Assuming T, b, x, y, z known, equations

$$\begin{aligned}(T_{11}-T_{31}x^*)x+(T_{12}-T_{32}x^*)y+(T_{13}-T_{33}x^*)z+(b_1-b_3x^*)=0,\\(T_{21}-T_{31}y^*)x+(T_{22}-T_{32}y^*)y+(T_{23}-T_{33}y^*)z+(b_2-b_3y^*)=0,\end{aligned} \quad (1)$$

can be used to model the photographing process itself. If x^*, y^*, x, y, z are known, then (1) represent two equations with 12 unknown elements T, b. Applying these equations to $n >= 6$ non-coplanar points in object space and to their images on a perspective projection, we obtain a homogeneous system of $2n$ equations with 12 unknowns. To solve the resulting system, we transfer the terms containing the normalization coefficient b_3 to the right and set the value $b_3 = 1$. Thus, to find the solution T, b, we obtain an overdetermined system of equations, the matrix of which we cannot invert, since it is not square. As is known from the theory of the

method of least squares, we can calculate the best-averaged solution by multiplying both sides of the matrix equation by the transposed matrix of the system. Then we get a system of 11 linear equations for 11 unknowns with a symmetric square matrix, for solving which we can apply the well-known square root method. Thus, by known coordinates, there is determined a transformation that gave rise to a given perspective projection, for example, a photograph.

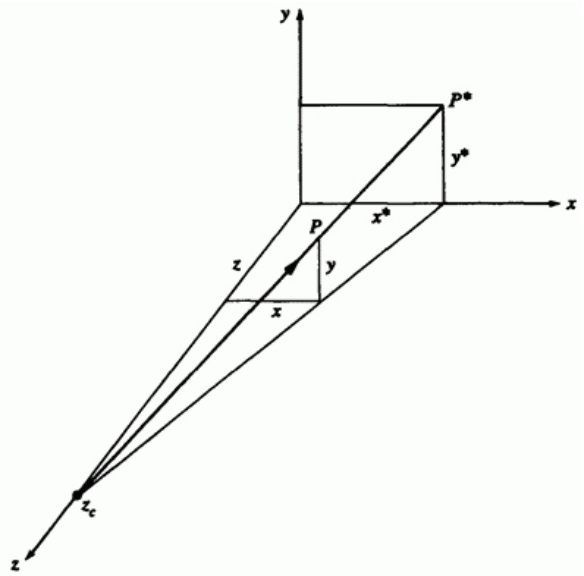

Figure 3. Perspective projection of the point

In the photogrammetry method, we use a stereo pair as the image of object, i.e. two projections of the same three-dimensional object, recorded in different angles [12]. In this case T, b, x^*, y^* are assumed known in equations (1). Then two equations are obtained from three unknown spatial coordinates x, y, z. This is an underdetermined system of equations, so it is impossible to solve it. However, if we know two perspective projections, say two photographs taken from different angles, then we can write these equations for both projections

$$\left(T_{11}^1 - T_{31}^1 x^{*1}\right)x + \left(T_{12}^1 - T_{32}^1 x^{*1}\right)y + \left(T_{13}^1 - T_{33}^1 x^{*1}\right)z = x^{*1} - b_1^1,$$
$$\left(T_{21}^1 - T_{31}^1 y^{*1}\right)x + \left(T_{22}^1 - T_{32}^1 y^{*1}\right)y + \left(T_{23}^1 - T_{33}^1 y^{*1}\right)z = y^{*1} - b_1^1,$$
$$\left(T_{11}^2 - T_{31}^2 x^{*2}\right)x + \left(T_{12}^2 - T_{32}^2 x^{*2}\right)y + \left(T_{13}^2 - T_{33}^2 x^{*2}\right)z = x^{*2} - b_1^1,$$
$$\left(T_{21}^2 - T_{31}^2 y^{*2}\right)x + \left(T_{22}^2 - T_{32}^2 y^{*2}\right)y + \left(T_{23}^2 - T_{33}^2 y^{*2}\right)z = y^{*2} - b_1^1.$$

As a result, we obtain four equations from three unknown spatial coordinates x, y, z, where superscripts [1] and [2] denote the first and second perspective projections. Thus, an overdetermined system of equations is again obtained, and the least squares and square root methods can be used to find the coordinates of the point x, y, z.

With the next movement of the camera, we obtain 11 new parameters; however, not all of them are independent. Namely, five parameters are responsible for the so-called internal parameters of the camera (focal lengths, the coordinates of the main point and the distortion parameter), which do not change when it is moved. To define them, we reduce the matrix of the projective transformation T to the upper triangular form, so that the result is the values of the angular and linear movements R, t of the camera

$$A = \begin{pmatrix} \alpha & \gamma & u_0 \\ 0 & \beta & v_0 \\ 0 & 0 & 1 \end{pmatrix}, \; R = A^{-1} \cdot T, t = A^{-1} \cdot b. \tag{2}$$

In fact, three Euler angles of rotation are in the matrix R. It is important that it is orthogonal. The application of the conditions of orthogonality makes the problem of determining the parameters R, t of the perspective transformation (external calibration) solvable, although nonlinear. Thus, it becomes possible to use $n >= 3$ calibration points of the object in space to construct the next calibration at perspective transformation. Recall

that it is these points on each image that the roadman is supposed to find to solve the problem of photogrammetry successfully.

In conditions when the internal parameters of the camera do not change, we have formulated a new "one-point" method of external calibration of the smartphone's camera. If we know the projective transform matrix T for the calibrated frame, we can fix the orientation angles of the smartphone's camera in the moment of internal calibration and the orientation angles for each stereopair frame: α, β, γ. After that we can get the rotation matrix of the second frame relative to the calibrated frame

$$P=\begin{pmatrix} \cos(\beta)\cos(\gamma) & -\cos(\alpha)\sin(\gamma)+\sin(\alpha)\sin(\beta)\cos(\gamma) & \cos(\gamma)\cos(\alpha)\sin(\beta)+\sin(\alpha)\sin(\gamma) \\ \sin(\gamma)\cos(\beta) & \cos(\alpha)\cos(\alpha)+\sin(\alpha)\sin(\beta)\sin(\gamma) & \sin(\beta)\cos(\alpha)\sin(\gamma)-\cos(\gamma)\sin(\alpha) \\ -\sin(\beta) & \sin(\alpha)\cos(\beta) & \cos(\beta)\cos(\alpha) \end{pmatrix},$$

where the resultant Euler angles α, β, γ of the rotation matrix are equal to the differences of the obtained angles. Then we calculate the projective transformation matrix T^2 for the second frame by the formula $T^2 = T^1 \cdot P$ and we find the coordinates of the normalized capture point vector for the second frame are from the equations:

$$b_1^2 = x^{*2} - (T_{11}^2 - T_{31}^2 x^{*2})x - (T_{12}^2 - T_{32}^2 x^{*2})y - \left(T_{13}^2 - T_{33}^2 x^{*2}\right)z,$$

$$b_2^2 = y^{*2} - (T_{21}^2 - T_{31}^2 y^{*2})x - (T_{22}^2 - T_{32}^2 y^{*2})y - \left(T_{23}^2 - T_{33}^2 y^{*2}\right)z.$$

Thus, the nonlinearity associated with the Euler angles disappears and the received solution allows performing 3D measurements on the smartphone at one single marker point. As in the previous example, one can use additional marker points – for later averaging.

The process of building a three-dimensional model for a set of pairs of corresponding points in a general case consists of five stages. 1. Calculation of the design matrix from measurements in the laboratory. 2. Calculation of the internal parameters of the camera according to the design matrix. 3. Video measurements on the object. 4. Calculation of external parameters. 5. The solution of the inverse problem for each pair of conjugate points. Moreover, knowing real points in space, you can calculate the parameters necessary for the certification of the defect of the road surface (area and volume).

2.1 Numerical experiment

For illustrating the method, we consider a real stereo pair, corresponding to two photographs of a typical road cone against the background of a hole in a road pavement (see figure 4). We measured the coordinates of the seven vertices of a 3D object with a ruler. In addition, we recorded the coordinates of the corresponding points on the images in a graphical editor using the mouse. Given the coordinates of the road surface point on the left and right images, one can estimate the accuracy of the presented technical vision algorithm. In our case, the distance from the tip of the cone to the asphalt coating calculated by the Pythagorean Theorem was 31.975 cm, which is 0.078% different from the 32 cm value on the technical data sheet.

Figure 4. Stereo pair: road cone against the background of damage to the road surface

The use of the “three-point” method, i.e. if we determined the internal parameters of the camera by all seven points, gave a value of 21.174 cm, which ensures a relative measurement error of 33.8%. However, the addition in this context of only one (i.e. fourth) point gave a value of 30.756 cm, which provides a quite acceptable relative measurement error of 3.8%. The performed numerical experiments allow us to recommend using such a device as a folding emergency stop sign, which has exactly four easily recognizable reference points, for video measurements on the object. A more responsible task of calibrating the internal parameters of the camera you can successfully perform in the laboratory on a much larger number of marker points, for example, in the Tsai

method [10] there are at least 25 of them. We emphasize that this requires the special care when performing measurement work. For example, for the previous example, the internal parameters of the camera on the left and right images do not match:

Table 1. Internal parameters of the camera in figure 4

Photo	α	β	u_0	v_0	γ
Left	795.578	642.85	794.579	841.311	15.669
Right	401.112	296.649	824.506	667.454	13.096

In the next series of experiments, there are 10 calibration points; including four corners of a label with a bar code (see figure 5). The internal parameters of the camera on the left and right images are equal, respectively:

Table 2. Internal parameters of the camera in figure 5

Photo	α	β	u_0	v_0	γ
Left	3599	3707	1340	2028	133.898
Right	3050	3233	981.91	2623	38.878

Then, for the 3D coordinates of the vertices of the dark tile next to the shaded area on the flooring, we get a perfectly acceptable result 9.757×3.738 instead of the expected values of 10×4.

Figure 5. Stereo pair of a packing box

2.2 On binarization of images at the pavement defects recognition

Further work consists in automating the process of searching for graphic markers and reference points on photographs. Allocation of object borders is the one of the most important tasks at pavement damages recognition. They contain exhaustive information on its form, for the subsequent analysis. The method of binarization of the initial image copes with this task. Nevertheless, in this process existence of a large number of distortions: washing out, gaps and loss of objects integrity, emergence of noise in homogeneous areas is characteristic. Demand of the mistakes elimination has led to emergence of a plenty of binarization methods.

Binarization process is transformation of the initial image to the image which elements can accept only two values. This process is need to the analysis of photos of pavement damages. Because it allows revealing objects, which contain the interesting information and it can execute their compact description. Creation of the automated systems of images recognition is a difficult theoretical and technical task. Development of new images binarization algorithms promotes finding the solution of the problems existing in the field of images recognition and in digital processing of images. The various approaches to images binarization exist. We can divide them onto two groups: the threshold methods and methods based on a brightness equality condition. In threshold methods, we seek for some characteristic (threshold) allowing dividing image elements on the two classes. The threshold can be constant or adaptive. The histogram of brightness values or entropy can be the basis of its choice. The Niblack's algorithm is the most known of nearby methods [13]. However, it badly copes with non-accurate structures in the field of a background. It was the reason of emergence of ideologically similar algorithms eliminating this defect. The Otsu method is one of the most effective threshold methods of binarization of grayscale images on quality and speed [14]. This method minimizes interclass dispersion.

Among the methods based on a condition of brightness equality, we can note Bayer's method [15]. This method uses ready binary templates with a different brightness. In addition, we can note the mistakes diffusion algorithm by Floyd-Steinberg [16], based on dithering (addition the noise before quantization). Its restrictive

feature is consistent implementation, because the result of processing of each following pixel depends on processing of previous.

In addition, we consider the new short-time binarization algorithm [17] in this report. This algorithm refers to methods, based on a condition of brightness equality. The main difference of this algorithm is enhancing contrast and allocating faint contrast details in grayscale images. The discrete shearlet transform (DST) [18] is one more method of the images binarization applying to the task. We use the "ShearLab" library by MATHLAB for building the DST [19].

The report shows a possibility of application of shearlet functions to the images binarization in the problem of pavement damages recognition. The figure 6 gives the example of the initial image containing pavement damage. The figure 7 and numbers in table 3 give results of binarization of the pavement damage image.

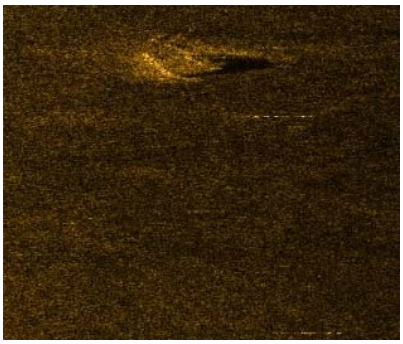

Figure 6. Image of the pavement damage

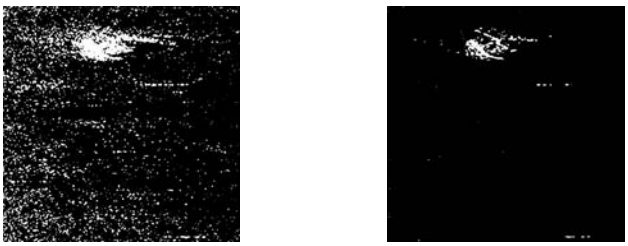

a) b)

Figure 7. Image of the pavement damage: a) 10% of significant coefficients, b) 1% of significant coefficients

Table 3. Estimation of image binarization quality (figures 6-7)

MAD (p=1)	RMSE (p=2)	PSNR (10%)	PSNR (1%)
0.3102	0.3909	19.44	18.08

In this article, we use the most common mathematical criteria for estimation of the image quality. The distance between two images $f = f(x, y)$ and $g = g(x, y)$ with dimensions $m \times n$ is defined by Hölder's norm, which is average on the quantity of image elements [17, 20]

$$d(f, g) = \|f - g\|_p = \left(\frac{1}{mn} \sum_{x=0}^{m-1} \sum_{y=0}^{n-1} |f(x, y) - g(x, y)|^p \right)^{1/p}, \; p \geq 1.$$

If $p = 1$ then we have the average difference (MAD). If $p = 2$ then we have the root by the standard deviation (RMSE).

Based on the distance we have the peak signal/noise relation (PSNR) between two images. It is determined

$$\mathrm{PSNR}(f, g) = 20 \cdot \lg \frac{2^k - 1}{\|f - g\|_2}.$$

We use the criteria of a minimum RMSE and a maximum PSNR to estimation of quality of the image processing.

Binarization allows reproducing details and borders of objects on images more precisely. Therefore, the accuracy of calculation of damage parameters increases. It is useful for data processing later on. As a preliminary conclusion, we note that on images of objects of artificial origin, for example, a pyramid or a cube,

at the vertices of which are graphic markers, the presence of angles formed by intersections of guidelines (curves or straight lines) are characteristic. Therefore, to analyze such images, it is advisable to use the so-called "corner" filters (Sobel, Laplacian, and Canny) [21-22]. For objects of natural origin, such as pits and potholes in the asphalt-concrete pavement, local inhomogeneities are characteristic; therefore, blob detectors are more suitable, based on the Laplace method [23]. Figures 8, 9 show the use of Harris detector for detecting conjugate points on left and right shots of stereopairs.

Figure 8. Stereopair of two photographs of the packaging box

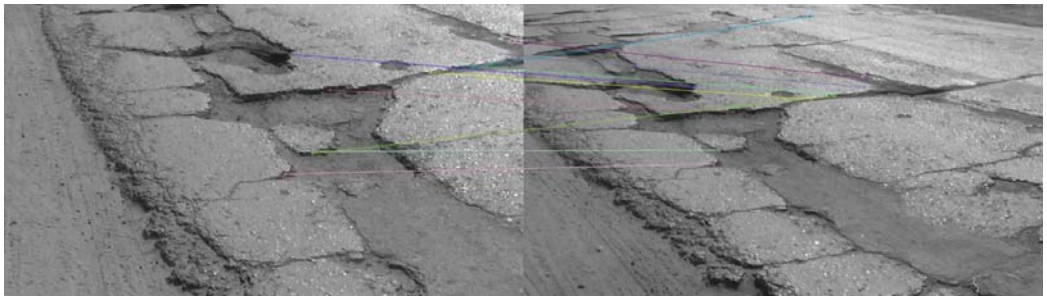

Figure 9. Stereopair of two photographs of the real pavement

3. The future works and discussion

We suppose to carry out the implementation of the obtained algorithms on a smartphone running the Android OS. Due to the peculiarities of the image of the defects of the roadway (lack of clear boundaries, the presence of outsiders objects, the insignificance of some defects), it should be possible to "manually" mark the characteristic points on the images. The algorithm for creating such an interface that allows selecting the characteristic points by the movement of the graphical cursor is the following. In succession, the left and then the right snapshot of the stereo pair are reset to the smartphone screen (figure 10, a). An image of a wire model of a 3D object superimposes the whole image. On the model, the characteristic points of the object flash, and the user by the movement of the graphic cursor selects the corresponding point in the photo. After processing both images of the stereo pair, the algorithm forms linear perspective transformation matrices in the smartphone's memory (a so-called calibration). Then by a command sent the user selects an arbitrary point in each snapshot of the stereo pair. It is proposed to choose from the appropriate menu the test mode (if it is a characteristic point belonging to the object), or the test mode for the probing of the Pythagorean Theorem (if it is a point on the road base), or to continue to work. Next, by a command sent the user selects the second point in each snapshot of the stereo pair; and the algorithm calculates the distance between selected points (another test). Next, the user selects the third and so on points in each picture of the stereo pair when prompted. As the array of characteristic points filled, it becomes possible using the triangulation technology to construct a three-dimensional mathematical model of a road surface defect. Then, based on the obtained model, the area and volume of the geometric figure that characterizes this particular damage to the road surface are calculated. A further task is to

prepare an order for the repair work to eliminate this road defect. The full cycle of works on the recognition of road surface damage is shown in figure 10, b.

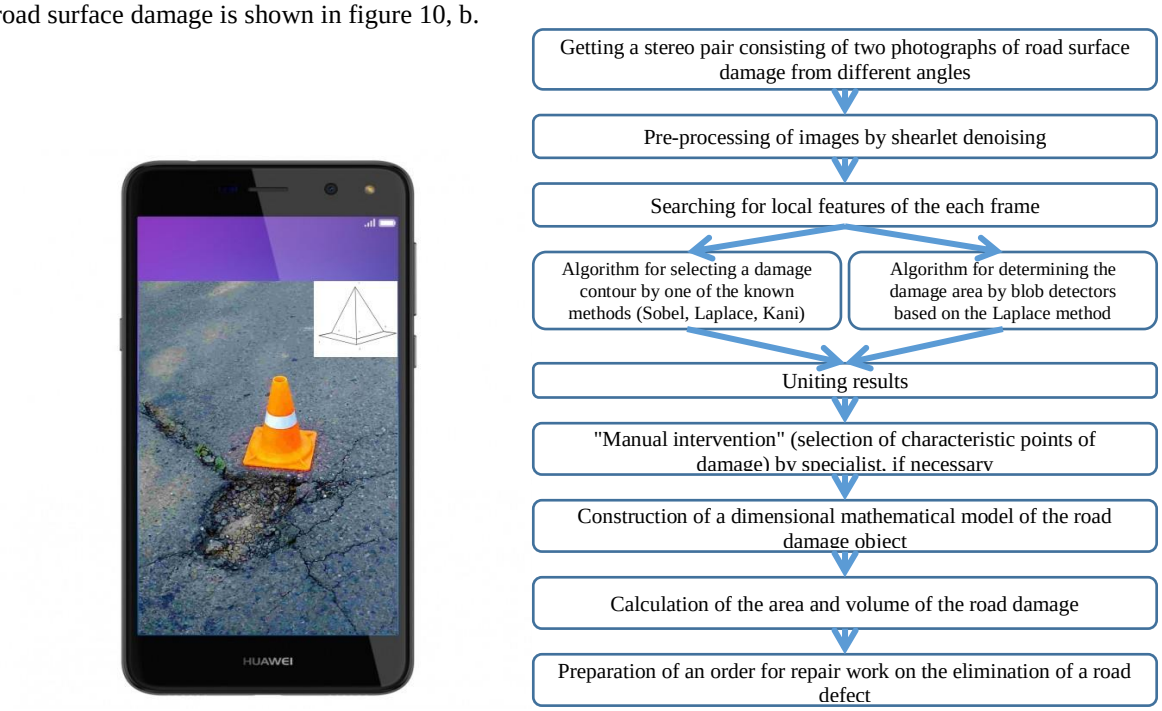

a) b)

Figure 10. a) Imitation of work with the image on the smartphone screen. b) The structure of the software-algorithmic complex recognition of road surface damage

The practical application of the algorithm stated in the report is quite wide, including when fixing and determining the actual dimensions of damage to vehicle based on the measured values of body surface points on the left and right images (figure 11). Examination of the nature and the list of damages to the vehicle provides for a detailed fixation of the damages to determine the possibility of their formation and involvement in the event under investigation. The corresponding act records the results of the visual inspection of the damaged vehicle and photographing. Photographs and inspection report for damaged car are a mandatory annex to the expert opinion or report on the assessment of the cost of repairing the car. Of course, the photogrammetric method is a weighty argument in solving controversial situations, and the determination of the actual size of damage to the elements of the car from photographs and video footage is an urgent task. In conclusion, we should say that the remote collection of data on road surface defects could be much more efficient using the methods described in this report. It is also worth considering the possibility of using epipolar geometry [24] and wavelets [25] to solve the problem.

Figure 11. Photos of a car damaged in a traffic accident

4. Acknowledgement

Research performed with the financial support of Russian Foundation for Basic Research and Tomsk oblast administration, grant No 16-41-700400 r_a.

5. References

[1] Domke E.R. Rassledovanie i jekspertiza dorozhno-transportnyh proisshestvij [Investigation and examination of road accidents]. Moscow: Akademija. 2009. (in Russian)
[2] Elugachev P., Shumilov B. Development of the technical vision algorithm. MATEC Web of Conferences, 216, 04003 (2018) / Polytransport Systems-2018: 7 p.
[3] Shumilov B.M., Esharov E. A., Arkabaev N. K. Construction and optimization of predictions on the basis of first-degree recurrence splines. Numerical Analysis and Applications, 3:2, 2010: p. 186-198.
[4] Bao G. Road distress analysis using 2D and 3D information. The University of Toledo: The University of Toledo Digital Repository Theses and Dissertations, 2010.
[5] Mezhenin A.V. Metody i sredstva raspoznavanija obrazov i vizualizacii [Methods and means of pattern recognition and visualization]. St. Petersburg: ITMO. 2012. (in Russian)
[6] Nazarov A.S. Fotogrammetrija [Photogrammetry]. Minsk: TetraSistems. 2006. (in Russian)
[7] Shumilov B.M., Baigulov A.N. A study on modeling of road pavements based on laser scanned data and a novel type of approximating hermite wavelets. WSEAS Transactions on Signal Processing, 11, 2015: p. 150-156.
[8] Chiuso A., Favaro P., Jin H., Soatto S. Structure from motion causally integrated over time. IEEE Trans. Pattern Anal. Machine Intell, 24, 2002: p. 523-535.
[9] Davison A.J., Reid I.D., Molton N.D., Stasse O. MonoSLAM: Real-Time Single Camera SLAM. IEEE Trans. Pattern Anal. Machine Intell, 29, 2007: p. 1052-1067.
[10] Tsai R. A versatile camera calibration technique for high-accuracy 3D machine vision metrology using off-the-shelf TV cameras and lenses. IEEE J. of Robotics and Automation, 3, 1987: p. 323-344.
[11] Rogers D.F., Adams J.A. Mathematical elements for computer graphics. New York: McGraw- Hill. 1990.
[12] Slama C. (ed.). Manual of Photogrammetry. American Society of Photogrammetry. Va.: Falls Church. 1980.
[13] Niblack W. An Introduce to Image Proccessing. NJ: Prentice-Hall, Enflewood Claiffs. 1986: p.115-116.
[14]Otsu N. A threshold selection method from gray-level histograms. IEEE Trans. on System, Man and Cybernetics, SMC-9:1, 1979: p. 62-66.
[15] Bayer B. An optimum method for two-level rendition of continuous tone pictures. IEEE International Conference on Communications, vol. 1, 1973: p. 11-15.
[16] Floyd R.W. An adaptive algorithm for spatial gray-scale. Proceedings Society Information Display, 17:2, 1976: p.75-78.
[17] Shumilov B., Gerasimova Y., Makarov A. On Binarization of Images at the Pavement Defects Recognition. 2018 IEEE International Conference on Electrical Engineering and Photonics (EExPolytech), Saint Petersburg, Russia, 2018: p. 107-110.
[18] Kutuniok G., Lim W.-Q., Steidl G. Shearlets: Theory and Applications. GAMM-Mitteilungen. 2014: 22 p.
[19] King E.J., Reisenhofer R., Kiefer J., Lim W.-Q., Li Z., Heygster G. Shearlet-Based Edge Detection: Flame Fronts and Tidal Flast. Applications of Digital Image Processing XXXVIII. 2015: 11 p.
[20] Wang Z., Bovik A.C. Modern Image Quality Assessment. New-York: Morgan and Claypool Publishing Company, 2006.
[21] Sonka M., Hlavac V., Boyle R. Image Processing. Analysis and Machine Vision. Thomson: Toronto. 2008.
[22] Harris affine region detector. Available at: https://en.wikipedia.org/wiki/ Harris_affine_region_detector (June 11, 2018)
[23] Tuytelaars T., Mikolajczyk K. Foundations and Trends in Computer Graphics and Vision, 3, 2007: p. 177-280.
[24] Hartley R., Zisserman A. Multiple View Geometry in Computer Vision. Second Edition. Cambridge: Cambridge University Press. 2004.
[25] Shumilov B.M. Multiwavelets of the third degree Hermitian splines, orthogonal to cubic polynomials. Mathematical models and computer simulations, 5:6, 2013: p. 511-519.